Uniqueness result for an inverse conductivity recovery problem with application to EEG

Maureen Clerc, Juliette Leblond, Jean-Paul Marmorat, Christos Papageorgakis

Rend. Istit. Mat. Univ. Trieste
Volume 47 (2015), 1–22 (electronic preview)

Uniqueness result for an inverse conductivity recovery problem with application to EEG

Maureen Clerc, Juliette Leblond,
Jean-Paul Marmorat and Christos Papageorgakis

Dedicated to Giovanni Alessandrini.

Abstract. *Considering a geometry made of three concentric spherical nested layers, each with constant homogeneous conductivity, we establish a uniqueness result in inverse conductivity estimation, from partial boundary data in presence of a known source term. We make use of spherical harmonics and linear algebra computations, that also provide us with stability results and a robust reconstruction algorithm. As an application to electroencephalography (EEG), in a spherical 3-layer head model (brain, skull, scalp), we numerically estimate the skull conductivity from available data (electrical potential at electrodes locations on the scalp, vanishing current flux) and given pointwise dipolar sources in the brain.*

Keywords: elliptic and Laplace-Poisson PDE, inverse conductivity recovery problem, spherical harmonics, EEG.
MS Classification 2010: 31B20, 33C55, 35J05, 35J25, 35Q61, 65R32, 92C55.

1. Introduction

We study an inverse conductivity recovery problem in the particular case of a spherical 3D domain Ω (a ball in $\mathbb{R}^3$) and for piecewise constant conductivity functions, of which one value is unknown. More precisely, we assume Ω to be made of 3 nested spherical layers, whose conductivity values are known in the innermost and outermost layers. We assume that the elliptic partial differential conductivity equation holds with a given source term in divergence form supported in the innermost layer.

Provided a single measurement as a pair of Cauchy data on the boundary (open subset of the sphere $\partial\Omega$), we will establish uniqueness and stability properties together with a reconstruction algorithm for the intermediate conductivity. We will also perform some analysis in order to investigate robustness of the reconstruction with respect to available measurements and sources in-

formation.

We face a very specific version of the many inverse conductivity issues for second order elliptic PDE under study nowadays. This one is related to piecewise constant conductivities in a spherical geometry in $\mathbb{R}^3$, and set from a single (Cauchy pair of partial) boundary measurement. Similar inverse conductivity recovery problems may be formulated in more general (Lipschitz smooth) domains of arbitrary dimension, with more general conductivities. They are often considered from (several or) infinitely many boundary measurements (pairs of Cauchy data, related Dirichlet-to-Neumann operator), and are called after Calderón, or after medical imaging processes (Electrical Impedance Tomography). Uniqueness and stability conductivity recovery issues are deeply discussed in [1, 2, 3, 6, 19, 29, 24].

More general inverse problems for elliptic PDEs, in particular transmission issues, are discussed in [20, 25]. Stability properties of Cauchy boundary value problems are described in [5] (see also references therein).

A fundamental problem in experimental neuroscience is the inverse problem of source localization, which aims at locating the sources of the electric activity of the functioning human brain using non-invasive measurements, such as electroencephalography (EEG), see [10, 14, 16, 17, 18, 21].

EEG measures the effect of the electric activity of active brain regions through values of the electric potential obtained by a set of electrodes placed at the surface of the scalp [14] and serves for clinical (location of epilepsy foci) and cognitive studies of the living human brain.

The inverse source localization problem in EEG is influenced by the electric conductivities of the several head tissues and especially by the conductivity of the skull [30]. The human skull is a bony tissue consisting of compact and spongy bone compartments, whose distribution and density varies across individuals, and according to age, since humidity of tissues, and therefore their conductivity tends to decrease [28]. Therefore conductivity estimation techniques are required to minimize the uncertainty in source reconstruction due to the skull conductivity.

Typically, an inverse conductivity estimation problem aims at determining an unknown conductivity value inside a domain Ω from measurements acquired on the boundary $\partial\Omega$. In the EEG case, the measurements can be modeled as pointwise values obtained on a portion of the boundary $\partial\Omega$ (the upper part of the scalp) but they are also affected by noise and measurement errors. The questions arising are: the uniqueness of the skull conductivity for known sources inside the brain; the stability of this estimation; and a constructive estimation method.

Quite frequently, for piecewise constant conductivities, the sub-domain (supporting the unknown conductivity value) is also to be determined, in some cases more importantly than the constant conductivity value itself (for example for

tumor detection, see [7, Ch. 3] and references therein, [22, 23]). But in the case of EEG, the sub-domains containing the various tissues can be considered known, because they can be extracted from magnetic resonance images. And for simplicity, we only consider the inverse skull conductivity estimation problem in a three-layer spherical head geometry, using partial boundary EEG data. The dipolar sources positions and moments will be considered to be known. This may appear to be an unrealistic assumption because sources reconstruction is itself a difficult inverse problem. But in fact, in some situations there are prior assumptions as to the positions of the sources (in primary evoked electrical potentials), and the position of a source also constrains its orientation, because to the laminar organization of pyramidal neurons in the grey matter.

The overview of this work is as follows. In Section 2, we precise the model and the considered inverse conductivity recovery issue. Our main uniqueness and stability results are stated and proved in Section 3, while an application to EEG and a numerical study are given in Section 4. We then provide a short conclusion in Section 5.

2. Model, problems

2.1. Domain geometry, conductivity

We consider the inverse conductivity estimation problem in a spherical domain $\Omega \subset \mathbb{R}^3$ made of 3 concentric spherical layers (centered at 0), a ball Ω_0, and 2 consecutive surrounding spherical shells Ω_1, Ω_2. Their respective boundaries are the spheres denoted as S_0, S_1, and S_2, with S_i of radius r_i such that $0 < r_0 < r_1 < r_2$. We also put $\Omega_3 = \mathbb{R}^3 \setminus \overline{\Omega} = \mathbb{R}^3 \setminus (\Omega \cup S_2)$.

For $i = 0, 1, 2$, we assume that σ is a real valued piecewise constant conductivity coefficient with values $\sigma_i > 0$ in Ω_i. Let also $\sigma_3 = 0$.

Note that in the present work, the values σ_i of the conductivity in Ω_i for $i \neq 1$ are assumed to be known.

In the EEG framework and for spherical three-layer head models, the domains Ω_i respectively represent the brain, the skull and the scalp tissues for $i = 0, 1, 2$, as shown in Figure 1, see [17, 18]. There, under isotropic assumption, it holds that $0 < \sigma_1 < \sigma_0 \simeq \sigma_2$.

Throughout the present work, the geometry Ω and the conductivity σ will be assumed to satisfy the above assumptions. More general situations are briefly discussed in Remark 3.2 and in Section 5.

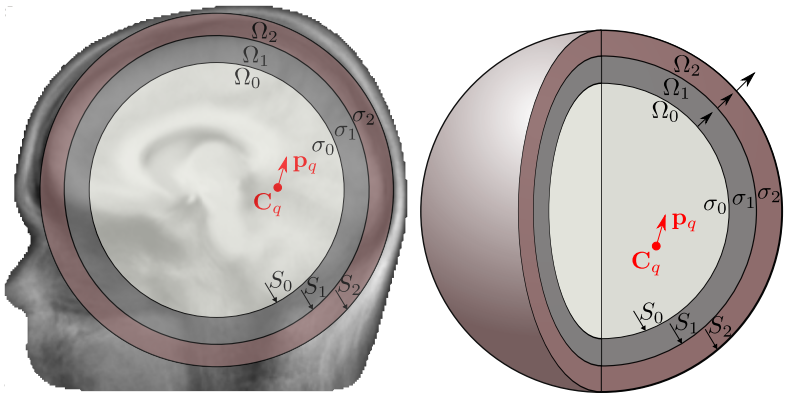

Figure 1: Spherical head model, with one source $\mathbf{C}_q$, $\mathbf{p}_q$.

2.2. Partial differential equations, source terms

We consider conductivity Poisson equations

$$\nabla \cdot \big(\sigma \nabla u\big) = \mathcal{S} \text{ or } \operatorname{div}\left(\sigma \operatorname{grad} u\right) = \mathcal{S} \text{ in } \mathbb{R}^3\,, \tag{1}$$

(in the distributional sense), with a source term $\mathcal{S}$ taken to be a distribution on $\mathbb{R}^3$ compactly supported in Ω_0.

We investigate situations where $\mathcal{S}$ is of divergence form:

$$\mathcal{S} = \nabla \cdot \mathbf{J}^P = \operatorname{div} \mathbf{J}^P\,,$$

for distributions $\mathbf{J}^P$ made of Q pointwise dipolar sources located at $\mathbf{C}_q \in \Omega_0$ with (non zero) moments $\mathbf{p}_q \in \mathbb{R}^3$:

$$\mathbf{J}^P = \sum_{q=1}^{Q} \mathbf{p}_q\, \delta_{\mathbf{C}_q}\,, \text{ whence } \mathcal{S} = \sum_{q=1}^{Q} \mathbf{p}_q \cdot \nabla \delta_{\mathbf{C}_q}\,, \tag{2}$$

where $\delta_{\mathbf{C}_q}$ is the Dirac distribution supported at $\mathbf{C}_q \in \Omega_0$. Therefore, in $\mathbb{R}^3$,

$$\nabla \cdot \big(\sigma \nabla u\big) = \sum_{q=1}^{Q} \mathbf{p}_q \cdot \nabla \delta_{\mathbf{C}_q}\,. \tag{3}$$

For the EEG case, under the quasi-static approximation and modeling the primary cerebral current $\mathbf{J}^P$ as in (2), Maxwell's equations imply that the conductivity PDE (3) drives the behaviour of the electric potential u [17].

2.3. Laplace-Poisson PDE and transmission conditions

For $i = 0, 1, 2, 3$, write $u_{|\Omega_i} = u_i$ for the restriction to Ω_i of the solution u to (3). We put $\partial_n u_i$ for the normal derivative of u_i on spheres in $\overline{\Omega}_i$, the unit normal vector being taken towards the exterior direction (pointing to Ω_{i+1}). In the present spherical setting, we actually have $\partial_n = \partial_r$.

For $i = 1, 2, 3$, the following transmission conditions hold on S_{i-1}, in particular in $L^2(S_{i-1})$, see [10, 14, 16] (and Section 2.5):

$$u_{i-1} = u_i\,, \quad \sigma_{i-1}\,\partial_n u_{i-1} = \sigma_i\,\partial_n u_i\,.$$

Linked by those boundary conditions, the solutions u_i to (3) in Ω_i satisfy the following Laplace and Laplace-Poisson equations:

$$\begin{cases} \Delta\, u_i = 0 \text{ in } \Omega_i\,,\ i > 0\,, \\ \Delta\, u_0 = \dfrac{1}{\sigma_0} \displaystyle\sum_{q=1}^{Q} \mathbf{p}_q \cdot \nabla \delta_{\mathbf{C}_q} \text{ in } \Omega_0\,. \end{cases} \tag{4}$$

We will see (in Section 3.2.2) that the transmission from $\begin{bmatrix} u_i \\ \partial_n u_i \end{bmatrix}$ on S_i to $\begin{bmatrix} u_{i-1} \\ \partial_n u_{i-1} \end{bmatrix}$ on S_{i-1}, for $i = 1, 2$, may be written

$$\begin{bmatrix} u_{i-1} \\ \partial_n u_{i-1} \end{bmatrix}_{|S_{i-1}} = \begin{bmatrix} 1 & 0 \\ 0 & \frac{\sigma_i}{\sigma_{i-1}} \end{bmatrix} \mathcal{T}(S_{i-1}, S_i) \begin{bmatrix} u_i \\ \partial_n u_i \end{bmatrix}_{|S_i}\,.$$

for some operator $\mathcal{T}(S_{i-1}, S_i)$ that accounts for the harmonicity of u_i in Ω_i and that we will express using spherical harmonics.

2.4. Inverse conductivity recovery problem

We consider the inverse conductivity estimation problem in the 3-layered spherical framework of Sections 2.1, 2.2.

From Cauchy data $u = g$ in an open subset Γ of $\partial\Omega = S_2$, and $\partial_n u = 0$ on S_2 and a (known) source term $\mathcal{S}$ given by (2), we want to recover the constant value σ_1 of the conductivity σ in the intermediate Ω_1 layer of a solution to (3) (or to (1), for more general source terms $\mathcal{S}$).

Below we establish uniqueness properties of σ_1 from Cauchy data u on $\Gamma \subset S_2$, $\partial_n u$ on S_2 and from the source term $\mathcal{S}$. A stability result is also given for $\Gamma = S_2$.

Provided (a single pair of non identically vanishing smooth enough) Cauchy boundary data u, $\partial_n u$ on $\Gamma \subset S_2$, whenever $\Gamma \neq \emptyset$ is open, uniqueness of u

holds on S_2, then on S_1 and S_0, as ensured by the formulation of Section 2.3 and Holmgren's theorem. It is enough to assume that $u \in W^{1,2}(\Gamma)$ (the Sobolev-Hilbert space of $L^2(\Gamma)$ functions with first derivative in $L^2(\Gamma)$) and $\partial_n u \in L^2(\Gamma)$, see [11, 13, 15].

Following Section 2.3, we face a preliminary data transmission issue from Γ to S_0, a Cauchy boundary value problem for Laplace equation, which needs to be regularized in order to be well-posed [20]. This is usually done by Thykonov regularization or the addition of an appropriate constraint and may be solved using boundary elements methods, see [8, 14] and references therein.

In EEG, data are provided as pointwise values of g at points in Γ (electrodes measurements), and yet another extension step is needed in order to compute an estimate of g on S_2, using best constrained approximation, see Section 4.

Note that a source term $\mathcal{S}$ only determines u_0 on S_0 up to the addition of a harmonic function in Ω_0. Indeed, by convolution with a fundamental solution of Laplace equation in $\mathbb{R}^3$, we see that

$$u_s(\mathbf{x}) = \frac{1}{4\pi} \sum_{q=1}^{Q} \frac{< \mathbf{p}_q, \mathbf{x} - \mathbf{C}_q >}{|\mathbf{x} - \mathbf{C}_q|^3} \, , \mathbf{x} \notin \{\mathbf{C}_q\} \, , \tag{5}$$

satisfies $u_s(\mathbf{x}) \to 0$ at $|\mathbf{x}| \to \infty$,

$$\Delta \, u_s = \sum_{q=1}^{Q} \mathbf{p}_q \cdot \nabla \delta_{\mathbf{C}_q} \, ,$$

in $\mathbb{R}^3$, whence in Ω and Ω_0, and $\Delta \, u_s = 0$ outside Ω_0. Solutions u_0 to (4) in Ω_0 are then provided by u_s/σ_0 up to the addition of a harmonic function in Ω_0. The later is in fact (uniquely) determined by the (transmitted) boundary conditions, see [10, Sec. 1.2], [14, 16, 21] where inverse source problems in the EEG setting are discussed, together with reconstruction algorithms.

2.5. Associated forward Neumann problem

Let $\phi \in L^2(S_2)$ (actually it is enough to take $\phi \in W^{-1/2,2}(S_2)$) of vanishing mean value on S_2. Then, there exists a solution u to (3) in Ω, Hölder continuous in $\overline{\Omega} \setminus \{\mathbf{C}_q\}$, which satisfies $\partial_n u = \phi$ on S_2; it is unique up to an additive constant. In particular, the associated Dirichlet boundary trace $u_{|S_2}$ is Hölder continuous on S_2. Indeed, looking to $u - u_s$ as a (weak) solution to a strictly elliptic PDE in a bounded smooth domain Ω or to a sequence of Laplace equations in the domains Ω_i, variational formulation and Lax-Milgram theorem imply that $u - u_s \in W^{1,2}(\Omega)$ and the uniqueness property, see [11, 13, 15]. Hence $u - u_s$ belongs to $W^{1/2,2}(S_2)$ and actually to $W^{1,2}(S_2)$. That u possesses

yet more regularity properties is established in [10, Prop. 1], see also [5] for stability results of Cauchy boundary transmission problems.

3. Conductivity recovery

3.1. Uniqueness result

Recall that the geometry Ω and the conductivity coefficients satisfy the hypotheses of Section 2.1. Let $\Gamma \subset S_2$ a (non empty) open set.

Assume the source term $\mathcal{S}$ given by (2) to be known, and not to be reduced to a single dipolar pointwise source located at the origin ($\mathcal{S} \neq \mathbf{p} \cdot \nabla \delta_{\mathbf{0}}$).

THEOREM 3.1. *Let σ, σ' be piecewise constant conductivities in Ω associated to two values σ_1, σ_1' in Ω_1 and equal values σ_0, σ_2 in Ω_0, Ω_2. If two solutions u, u' to (3) associated with σ, σ' and such that $\partial_n u = \partial_n u' = 0$ on S_2 coincide on Γ: $u_{|\Gamma} = u'_{|\Gamma} \not\equiv 0$, then $\sigma_1 = \sigma_1'$.*

This implies that a single pair of partial boundary Dirichlet data $u_{|\Gamma}$ on Γ and Neumann data $\partial_n u = 0$ (vanishing) on S_2 of a solution u to (3) uniquely determines $\sigma_1 > 0$.

Note that Theorem 3.1 also holds true for non identically vanishing Neumann on $\Gamma \subset S_2$. We will discuss more general statements of this result in Remark 3.2 below, after the proof, see also Section 5.

In order to establish the result, we use spherical harmonics expansions that we now precise.

3.2. Spherical harmonics expansions

In order to express harmonic functions in the spherical shells and balls Ω_i and their boundary values on S_i, we use the spherical harmonics basis $r^k\, Y_{km}(\theta, \varphi)$, $r^{-(k+1)}\, Y_{km}(\theta, \varphi)$, $k \geq 0$, $|m| \leq k$, in the spherical coordinates (r, θ, φ). These are homogeneous harmonic and anti-harmonic polynomials for which we refer to [9, Ch. 9, 10],[15, Ch. II, Sec. 7.3] as for their properties. (the basis functions $Y_{km}(\theta, \varphi)$ are products beteween associated Legendre functions of indices $k \geq 0$, $|m| \leq k$, applied to $\cos\theta$ and elements of the Fourier basis of index m on circles in φ (real or complex valued, $\cos m\varphi$, $\sin m\varphi$ or $e^{\pm im\varphi}$).

3.2.1. Source term, boundary data

The decomposition theorem [9, Thm 9.6], [15, Ch. II, Sec. 7.3, Prop. 6], is to the effect that the restriction u_i of u to Ω_i for $i = 1, 2$ may be expanded on the

spherical harmonics basis as follows, at $(r,\theta,\varphi) \in \Omega_i$:

$$u_i(r,\theta,\varphi) = \sum_{k=0}^{\infty} \sum_{m=-k}^{k} \left[\alpha_{ikm} r^k + \beta_{ikm} r^{-(k+1)}\right] Y_{km}(\theta,\varphi)\,, \tag{6}$$

where α_{ikm} and β_{ikm} are the spherical harmonic coefficients of the harmonic and anti-harmonic parts of u_i, respectively (harmonic inside or outside $\cup_{j\leq i}\Omega_i$). Similarly, because it is harmonic in a spherical layer surrounding S_0, the restriction u_0 of u to Ω_0 is given at points (r,θ,φ) with $r > \max_q |\mathbf{C}_q| > 0$ by

$$u_0(r,\theta,\varphi) = \sum_{k=0}^{\infty} \sum_{m=-k}^{k} \alpha_{0km} r^k\, Y_{km}(\theta,\varphi) + u_s(r,\theta,\varphi)\,,$$

where u_s given by (5) is expanded there (and at $r \neq 0$) as:

$$u_s(r,\theta,\varphi) = \sum_{k,m} \beta_{0km} r^{-(k+1)} Y_{km}(\theta,\varphi)\,. \tag{7}$$

Here, β_{0km} are the spherical harmonic coefficients of the anti-harmonic (harmonic outside Ω_0) function u_S.

The normal derivative of u_i, $i = 0,1,2$, is then given in Ω_i (with $r > \max_q |\mathbf{C}_q|$ for $i = 0$) by:

$$\partial_n u_i(r,\theta,\varphi) = \sum_{k,m} \left[\alpha_{ikm} k r^{k-1} - \beta_{ikm}(k+1) r^{-(k+2)}\right] Y_{km}(\theta,\varphi) \tag{8}$$

On S_i, we put (because $u_i \in L^2(S_i)$ where the spherical harmonics form an orthogonal basis [9, Thm 5.12]):

$$u_i(r_i,\theta,\varphi) = \sum_{k=0}^{\infty} \sum_{m=-k}^{k} \gamma_{ikm} Y_{km}(\theta,\varphi)\ ,\ \partial_n u_i(r_i,\theta,\varphi) = \sum_{k=0}^{\infty} \sum_{m=-k}^{k} \delta_{ikm} Y_{km}(\theta,\varphi)\ ,$$

with l^2 summable coefficients γ_{ikm}, δ_{ikm} (that may be real or complex valued depending on the choice for Y_{km}).

In particular, once the boundary data $u_2 = g$ is extended from Γ to S_2 (see [8, 14] and the discussion in Section 2.4), we have:

$$u_2(r_2,\theta,\varphi) = \sum_{k,m} \gamma_{2km} Y_{km}(\theta,\varphi) = \sum_{k,m} g_{km} Y_{km}(\theta,\varphi)\,,$$

with $g_{km} = \gamma_{2km}$, whereas the corresponding $\delta_{2km} = 0$ since $\partial_n u_2 = 0$ on S_2 (because $\sigma_3 = 0$).

3.2.2. Preliminary computations

Below, we write for sake of simplicity, for $i = 0, 1, 2$: $\alpha_{ik} = \alpha_{ikm}$, $\beta_{ik} = \beta_{ikm}$, $\gamma_{ik} = \gamma_{ikm}$, $\delta_{ik} = \delta_{ikm}$, $g_{km} = g_k$, for all $k \geq 0$, and every $|m| \leq k$ (we could also take the sums over $|m| \leq k$).

Recall from Section 2.3 that the following transmission conditions hold on S_{i-1} for $i = 1, 2, 3$:

$$\Sigma_{i-1} \begin{bmatrix} u_{i-1} \\ \partial_n u_{i-1} \end{bmatrix}_{|S_{i-1}} = \Sigma_i \begin{bmatrix} u_i \\ \partial_n u_i \end{bmatrix}_{|S_{i-1}}, \tag{9}$$

with

$$\Sigma_i = \begin{bmatrix} 1 & 0 \\ 0 & \sigma_i \end{bmatrix} \text{ hence } \Sigma_i^{-1} = \begin{bmatrix} 1 & 0 \\ 0 & \frac{1}{\sigma_i} \end{bmatrix} \text{ and } \sigma_i \, \Sigma_i^{-1} = \begin{bmatrix} \sigma_i & 0 \\ 0 & 1 \end{bmatrix}.$$

By projection of (6), (8), onto (the orthogonal $L^2(S_i)$ basis of) spherical harmonics, and with

$$T_k(r_i) = \begin{bmatrix} r_i^k & r_i^{-(k+1)} \\ k r_i^{k-1} & -(k+1) r_i^{-(k+2)} \end{bmatrix},$$

we obtain for all $k \geq 0$ the following relations on S_i:

$$\begin{bmatrix} \gamma_{ik} \\ \delta_{ik} \end{bmatrix} = T_k(r_i) \begin{bmatrix} \alpha_{ik} \\ \beta_{ik} \end{bmatrix}.$$

In particular:

$$\beta_{ik} = \frac{r_i^{k+1}}{2k+1} \left(k \, \gamma_{ik} - \delta_{ik} \right). \tag{10}$$

The transmission conditions (9) through S_{i-1} express as:

$$\Sigma_{i-1} \begin{bmatrix} \gamma_{i-1k} \\ \delta_{i-1k} \end{bmatrix} = \Sigma_i \, T_k(r_{i-1}) \begin{bmatrix} \alpha_{ik} \\ \beta_{ik} \end{bmatrix}.$$

Because $T_k(r_i)$ is invertible ($r_i > 0$), this implies that:

$$\begin{bmatrix} \gamma_{i-1k} \\ \delta_{i-1k} \end{bmatrix} = \Sigma_{i-1}^{-1} \, \Sigma_i \, T_k(r_{i-1}) \, T_k(r_i)^{-1} \begin{bmatrix} \gamma_{ik} \\ \delta_{ik} \end{bmatrix}.$$

Therefore, in the spherical geometry, $\mathcal{T}(S_{i-1}, S_i) = T_k(r_{i-1}) \, T_k(r_i)^{-1}$ for the operator $\mathcal{T}(S_{i-1}, S_i)$ introduced at the end of Section 2.3.

Hence, because $\gamma_{2k} = g_k$ and $\delta_{2k} = 0$:

$$\begin{bmatrix} \delta_{0k} \\ \gamma_{0k} \end{bmatrix} = \Sigma_0^{-1}\, \Sigma_1\, T_k(r_0)\, T_k(r_1)^{-1}\, \Sigma_1^{-1}\, \Sigma_2\, T_k(r_1)\, T_k(r_2)^{-1} \begin{bmatrix} g_k \\ 0 \end{bmatrix}, \tag{11}$$

while

$$\beta_{0k} = [0\ 1]\, T_k(r_0)^{-1} \begin{bmatrix} \delta_{0k} \\ \gamma_{0k} \end{bmatrix}. \tag{12}$$

These formula express a linear relation between the source term coefficients β_{0k} and the boundary Dirichlet data with coefficients g_k, which is studied in Appendix and gives rise to (13) below. We already see the particular role of σ_1 that appears through Σ_1^{-1} and Σ_1. This explains why, after multiplication by σ_1 and algebraic manipulations, we obtain in (13) a polynomial of degree 2 in σ_1.

3.2.3. Algebraic equations

As computed in Appendix, equations (11), (12) can be rewritten, for all $k \geq 0$, as:

$$B_1(k)\, \sigma_1\, \beta_{0k} = \left(A_2(k)\, \sigma_1^2 + A_1(k)\, \sigma_1 + A_0(k)\right)\, g_k\,, \tag{13}$$

with non negative quantities $A_i(k)$, $i = 0, 1, 2$, $B_1(k)$ that depend only on the geometry, on the given conductivity values σ_0, σ_2, and on k. Actually, $A_1(k), B_1(k) > 0$ for all $k \geq 0$ while $A_0(k), A_2(k) > 0$ for $k > 0$ but $A_0(0) = A_2(0) = 0$. In particular, for all $k \geq 0$ and for $\sigma_1 > 0$, we have $A_2(k)\, \sigma_1^2 + A_1(k)\, \sigma_1 + A_0(k) > 0$.

This implies that $\beta_{0k} = 0 \Leftrightarrow g_k = 0$ and that for all k such that $g_k \neq 0$, β_{0k}/g_k is real valued positive: the spherical harmonics basis diagonalizes the transmission relations.

3.3. Uniqueness proof

Proof. (Theorem 3.1) Assume that there exists another value $\sigma_1' > 0$ of the conductivity in Ω_1 that gives rise to the same potential (and vanishing current flux) on $\Gamma \subset S_2$, from the same source term u_s (same boundary measurements and coefficients $g_k = g_{km}$, same sources term coefficients $\beta_{0k} = \beta_{0km}$, given). Equation (13) then holds for both $\sigma_1, \sigma_1' > 0$. We thus get that either $\beta_{0k} = g_k = 0$ or

$$\frac{\beta_{0k}}{g_k} = \frac{A_2(k)\, \sigma_1^2 + A_1(k)\, \sigma_1 + A_0(k)}{B_{1,k}\, \sigma_1} = \frac{A_2(k)\, \sigma_1'^2 + A_1(k)\, \sigma_1' + A_0(k)}{B_{1,k}\, \sigma_1'},$$

whence

$$\frac{A_2(k)\,\sigma_1^2 + A_1(k)\,\sigma_1 + A_0(k)}{B_{1,k}\,\sigma_1} - \frac{A_2(k)\,\sigma_1'^{,2} + A_1(k)\,\sigma_1' + A_0(k)}{B_{1,k}\,\sigma_1'} = 0\,,$$

hence multiplying by $B_{1,k}\,\sigma_1\,\sigma_1' > 0$:

$$(\sigma_1 - \sigma_1')\,(A_2(k)\,\sigma_1\,\sigma_1' - A_0(k)) = 0\,.$$

Thus either $\sigma_1' = \sigma_1$ and uniqueness holds or, for all values of $k \geq 0$ such that $\beta_{0k} \neq 0$,

$$A_0(k) = \sigma_1\,\sigma_1'\,A_2(k)\,.$$

This holds for $k = 0$ but for $k > 0$ it implies that

$$\frac{A_0(k)}{A_2(k)} = \sigma_1\,\sigma_1'\,,$$

which could not be true for more than a single value of $k > 0$. Indeed, the product $\sigma_1\,\sigma_1'$ is constant while $A_0(k)/A_2(k)$ stricly increases with k, as we now show. We have:

$$\frac{A_0(k)}{A_2(k)} = \sigma_0\,\sigma_2\,k\,\frac{1 - \left(\frac{r_1}{r_2}\right)^{2k+1}}{(k+1)\,\left(\frac{r_1}{r_2}\right)^{2k+1} + k} = \sigma_0\,\sigma_2\,k\,\frac{1 - \varrho^{2k+1}}{(k+1)\,\varrho^{2k+1} + k}\,, \qquad (14)$$

with $\varrho = r_1/r_2 < 1$, and we put:

$$E(k) = \frac{1}{\sigma_0\,\sigma_2}\frac{A_0(k)}{A_2(k)} = \frac{1 - \varrho^{2k+1}}{1 + \frac{k+1}{k}\,\varrho^{2k+1}}\,,\ k > 0\,,\ E(0) = 0\,.$$

Because for $k > 0$, $k + 2/(k+1) < (k+1)/k$ and $\varrho^{2k+3} < \varrho^{2k+1}$, the numerator of $E(k)$ strictly increases with k while its denominator strictly decreases. Thus, E is a strictly increasing function of k, which converges to 1 as $k \to \infty$.

Hence, among the $k > 0$, the equation $E(k) = \frac{\sigma_1\sigma_1'}{\sigma_0\,\sigma_2}$ admits at most one solution, and pairs $\sigma_1, \sigma_1' > 0$ cannot solve $A_2(k)\sigma_1\sigma_1' - A_0(k) = 0$ for more than 1 value of $k > 0$ (actually, a necessary condition for σ_1, σ_1' to solve $A_2(k)\sigma_1\sigma_1' - A_0(k) = 0$ for 1 value of $k > 0$ is that $\sigma_1\,\sigma_1' \in (0\,,\ \sigma_0\,\sigma_2)$). So we must have $\sigma_1' = \sigma_1$, as soon as β_{0k} (or g_k) does not vanish for at least 2 distinct values of k.

Finally, we show that potentials u_s associated to pointwise dipolar source terms $\mathcal{S} \neq \mathbf{p} \cdot \nabla\delta_{\mathbf{0}}$ have at least 2 non-null coefficients β_{0k} in their spherical harmonic expansion. Indeed, assume that all the coefficients β_{0km} are 0, except

for a single value of $k > 0$, say k_0. From (7), the function u_s is then a anti-harmonic homogeneous polynomial of degree k_0 and for $r > \max_q |\mathbf{C}_q| > 0$,

$$u_s(r,\theta,\varphi) = \sum_{|m|\leq k_0} \beta_{0k_0m} r^{-(k_0+1)} Y_{k_0m}(\theta,\varphi)$$

$$= \frac{1}{r^{2k_0+1}} \sum_{|m|\leq k_0} \beta_{0k_0m} r^{k_0} Y_{k_0m}(\theta,\varphi)\,.$$

From [9, Ch. 5], the distribution $\mathcal{S} = \Delta u_s$ also coincides far from $\{0\}$ with a polynomial divided by an odd power of r. This contradicts the assumptions on $\mathcal{S}$, which has a pointwise support in Ω_0 not reduced to $\{0\}$. □

REMARK 3.2. *Theorem 3.1 is in fact valid for solutions to Equation* (1) *with more general source terms $\mathcal{S}$. To ensure uniqueness, it is indeed enough to assume that u_s does not coincide with some homogeneous anti-harmonic polynomial of positive degree, so that it admits on S_0 at least two coefficients $\beta_{0k} \neq 0$.*

In the present spherical geometry, note that u_s is equal on S_0 to a homogeneous harmonic polynomial if and only if so is u on S_2.

The last part of the proof actually implies that potentials u_s issued from pointwise dipolar source terms $\mathcal{S}$ with support in Ω_0 not reduced to $\{0\}$ have infiniteley many coefficients $\beta_{0k} \neq 0$.

3.4. Stability properties

We now establish a stability result for the inverse conductivity estimation problem with respect to the source term whenever $\Gamma = S_2$.

PROPOSITION 3.3. *Assume the source terms $\mathcal{S}$, $\mathcal{S}'$ and the conductivities σ, σ' to satisfy the assumptions of Theorem 3.1. Let u_s, u'_s be the associated potentials through (5). Let u, u' be the associated solutions to* (3) *such that $\partial_n u = \partial_n u' = 0$ on S_2. Put g, g' for their boundary values on S_2. Then, there exist c, $c_s > 0$ such that*

$$|\sigma_1 - \sigma'_1| \leq c\,\|g - g'\|_{L^2(S_2)} + c_s\,\|u_s - u'_s\|_{L^2(S_0)}\,.$$

Whenever $0 < s_m \leq \sigma_1\,,\ \sigma'_1 \leq s_M$ for constants s_m, s_M, then c, c_s do not depend on $\sigma_1\,,\ \sigma'_1$ but on s_m, s_M (and on $\mathcal{S}$, through $\|g\|_{L^2(S_2)}$).

REMARK 3.4. *For ordered lists of sources $(\mathbf{p}_q, \mathbf{C}_q)$, $(\mathbf{p}'_q, \mathbf{C}'_q)$ with length Q, we can define the geometric distance*

$$d(\mathcal{S},\mathcal{S}') = \sum_{q=1}^{Q} \left(|\mathbf{p}_q - \mathbf{p}'_q| + |\mathbf{C}_q - \mathbf{C}'_q|\right)\,.$$

If points source are far enough from S_0 in the sense that $\max(|\mathbf{C}_q|, |\mathbf{C}'_q|) \leq \rho < r_0$*, and because u_s is on S_0 a continuous function of $\mathbf{p}_q, \mathbf{C}_q$, we can rewrite the inequality in Proposition 3.3 as:*

$$|\sigma_1 - \sigma'_1| \leq c \, \|g - g'\|_{L^2(S_2)} + c'_s \; d(\mathcal{S}, \mathcal{S}') \, ,$$

with $c'_s = K(\rho)\, c_s$ for some constant $K(\rho)$ which depends on ρ. Hence, the conductivity σ_1 depends continuously on the (complete) Dirichlet boundary data g (in $L^2(S_2)$) and on the source term $\mathcal{S}$, with appropriate topology. Note also the relation:

$$\beta_{0km} = \frac{1}{2k+1} \sum_{q=1}^{Q} \langle \mathbf{p}_q \, , \, \nabla \left(r^k \, Y_{km}(\theta, \varphi) \right) (\mathbf{C}_q) \rangle_{L^2(S_0)} \, .$$

Proof. Let

$$\varepsilon_k(\sigma_1, \beta_{0k}, g_k) = B_1(k)\, \sigma_1 \, \beta_{0k} - \left(A_2(k)\, \sigma_1^2 + A_1(k)\, \sigma_1 + A_0(k) \right) \, g_k \, , \qquad (15)$$

From $\sigma'_1 \, \varepsilon_k(\sigma_1, \beta_{0k}, g_k) - \sigma_1 \, \varepsilon_k(\sigma'_1, \beta'_{0k}, g'_k) = 0$, we get

$$0 = \sigma'_1 \, \varepsilon_k(\sigma_1, \beta_{0k} - \beta'_{0k}, g_k - g'_k) + \sigma'_1 \, \varepsilon_k(\sigma_1, \beta'_{0k}, g'_k) - \sigma_1 \, \varepsilon_k(\sigma'_1, \beta'_{0k}, g'_k) \, .$$

But

$$\sigma'_1 \, \varepsilon_k(\sigma_1, \beta'_{0k}, g'_k) - \sigma_1 \, \varepsilon_k(\sigma'_1, \beta'_{0k}, g'_k) = g'_k(\sigma_1 - \sigma'_1) \left[A_2(k) \sigma_1 \sigma'_1 - A_0(k) \right] \, ,$$

so

$$\begin{aligned} & g'_k(\sigma_1 - \sigma'_1) \left[A_2(k) \sigma_1 \sigma'_1 - A_0(k) \right] \; = \\ & \quad - \sigma'_1 \left[B_1(k) \sigma_1 (\beta_{0k} - \beta'_{0k}) - (A_2(k) \sigma_1^2 + A_1(k) \sigma_1 + A_0(k))(g_k - g'_k) \right] \, . \end{aligned}$$

Recall that $A_2(k) > 0$ for $k > 0$ and other arguments of Section 3.3 together with the computations in Appendix show that $A_0(k)/A_2(k)$, $A_1(k)/A_2(k)$, $r_0^{k+1} \, B_1(k)/A_2(k)$ are uniformely bounded in k from above and from below (by strictly positive constants). We can then divide by $A_2(k)$, in order to obtain

$$\begin{aligned} & |\sigma_1 - \sigma'_1| \, \left[\sum_{k,m} |g'_k|^2 \left| \sigma_1 \, \sigma'_1 - \frac{A_0(k)}{A_2(k)} \right|^2 \right]^{\frac{1}{2}} \\ & \leq \sqrt{2} \, \sigma'_1 \left[\sum_{k,m} \left(\sigma_1^2 + \frac{A_1(k)}{A_2(k)} \, \sigma_1 + \frac{A_0(k)}{A_2(k)} \right)^2 \, |g_k - g'_k|^2 \right]^{\frac{1}{2}} \\ & \quad + \sqrt{2} \, \sigma_1 \, \sigma'_1 \left[\sum_{k,m} \frac{B_1^2(k)}{A_2^2(k)} \, |\beta_{0k} - \beta'_{0k}|^2 \right]^{\frac{1}{2}} \, . \end{aligned}$$

In order to establish an upper bound, note that

$$\sum_{k,m} \frac{B_1^2(k)}{A_2^2(k)} \, |\beta_{0k} - \beta'_{0k}|^2 \leq \sup_k \frac{r_0^{2(k+1)} \, B_1^2(k)}{A_2^2(k)} \sum_{k,m} r_0^{-2(k+1)} \, |\beta_{0k} - \beta'_{0k}|^2 \, ,$$

with

$$\sum_{k,m} r_0^{-2(k+1)} \, |\beta_{0k} - \beta'_{0k}|^2 = \|u_s - u'_s\|^2_{L^2(S_0)} \, .$$

Moreover, since g_k (as β_{0k}) possess non vanishing values for infinitely many (at least two) values of k, and $\sigma_1 \, \sigma'_1 - A_0(k)/A_2(k)$ can vanish for at most one value of k, it holds that:

$$\sum_{k,m} |g'_k|^2 \, |\sigma_1 \, \sigma'_1 - A_0(k)/A_2(k)|^2 > 0 \, ,$$

can be bounded from below under the assumptions on $\sigma_1 \, \sigma'_1$. □

4. Application to EEG

In order to illustrate Proposition 3.3, we now perform a short numerical analysis of the inverse conductivity estimation problem in the spherical domain and the EEG setting described in Section 2. Measurements of the Dirichlet data g on the scalp S_2 (pointwise values at electrodes locations) and known sources activity are expanded on the spherical harmonics basis, using the FindSources3D software[1] (FS3D), see also [14]. We therefore have at our disposal the spherical harmonics coefficients (g_{km}, β_{0km}) for $0 \leq k \leq K$ for some $K > 0$ and $|m| \leq k$.

4.1. Reconstruction algorithm

As the reconstruction of the conductivity σ_1 does not depend on the spherical harmonics indices m, in order to increase the robustness of our reconstruction algorithm, the following normalization is applied over the different spherical harmonics indices k:

$$\begin{cases} \tilde{g}_k = \sum\limits_{|m| \leq k} g_{km} \, \bar{\beta}_{0km} \, , \\ \tilde{\beta}_{0k} = \sum\limits_{|m| \leq k} \beta_{0km} \, \bar{\beta}_{0km} = \sum\limits_{|m| \leq k} |\beta_{0km}|^2 \, . \end{cases}$$

There, $\bar{\beta}_{0km}$ is the complex conjugate number to β_{0km} (indeed, β_{0km} could be complex valued if the basis elements Y_{km} are taken in their complex valued form).

[1] See http://www-sop.inria.fr/apics/FindSources3D/.

The procedure is a least square minimization of the error equation obtained from (15) as a truncated finite sum for $K > 0$:

$$\sigma_1^{est} \;=\; \arg\min_s \sum_{k=0}^{K} \left| \varepsilon_k(s, \tilde{\beta}_{0k}, \tilde{g}_k) \right|^2 . \tag{16}$$

4.2. Numerical illustrations

We consider the EEG framework in the spherical three-layer head model, as described in Section 2.1, where the layers represent the brain, the skull and the scalp tissues, respectively. The radii of the spheres used in the numerical analysis are normalized to the values $r_0 = 0.87$, $r_1 = 0.92$ and $r_2 = 1$. In the present analysis, the brain and scalp tissue conductivities are set to $\sigma_0 = \sigma_2 = 0.33\,\mathrm{S/m}$, while the skull conductivity σ_1 is to be recovered. When generating simulated EEG data through the associated forward simulation, we will set $\sigma_1 = 0.0042\,\mathrm{S/m}$.

Our study uses simulated data associated to a single dipole and the minimization of (16) for the conductivity estimation. The algorithm is written as a MATLAB code and the forward simulations are run with the FS3D software.

We validate our reconstruction algorithm using simulated EEG data by FS3D (for solving the direct EEG problem). Of course, the EEG data are subject to some ambient noise and measurements errors, and the a priori knowledge on the sources is not perfect. The inverse conductivity estimation problem is sensitive to such perturbations though it possesses the stability property described in Proposition 3.3.

To investigate the stability of our algorithm with respect to the source term, we select a source term $\mathcal{S}$ made of a single dipole located at $\mathbf{C}_1 = (0.019, 0.667, 0.1)$, mimicking an EEG source at the frontal lobe of the brain, with moment $\mathbf{p}_1 = (0.027, 0.959, 0.28)$. The associated spherical harmonics coefficients $\tilde{g}_k$ and $\tilde{\beta}_{0k}$ are computed for $0 \le k \le K = 30$. The original source location $\mathbf{C}_1$ is replaced by inexact locations $\mathbf{C}_1^n$ for $n = 1, \cdots, 20$ located at a constant distance from $\mathbf{C}_1$ (a percentage of the inner sphere radius r_0), as illustrated in Figure 2, while the source moment $\mathbf{p}_1$ is retained. For each new dipole location $\mathbf{C}_1^n$, the associated spherical harmonics coefficients $\tilde{\beta}_{0k}^n$ are simulated. We perform conductivity estimation from the pairs $\tilde{g}_k$, $\tilde{\beta}_{0k}^n$ (recall that $\tilde{g}_k$ correspond to the actual $\tilde{\beta}_{0k}$).

The effect of the source mislocation on the conductivity estimation is summarized in Figure 3 and Table 4.2 which respectively shows and lists the values and other characteristics of the estimated conductivities with respect to the distance between actual and inexact sources.

These preliminary results illustrate the influence of source mislocation on conductivity estimation, and the robustness character of our algorithm, in ac-

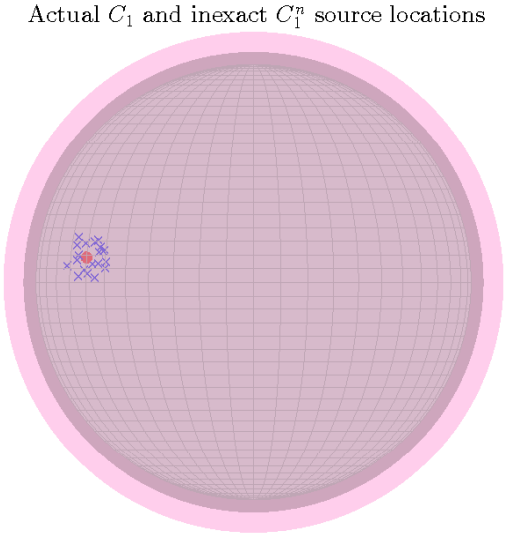

Figure 2: Locations (in Ω_0) of $\mathbf{C}_1$ (red bullet) and of the 20 points $\mathbf{C}_1^n$ (blue cross) surrounding it, for $|\mathbf{C}_1 - \mathbf{C}_1^n|$ equal to 10% of r_0.

Dipole mislocation (% of radius r_0)	$\tilde{\sigma}_1^{est}$	Standard deviation	Mean of relative errors
0	4.200e-03	0	1.858e-15
0.1	4.195e-03	1.450e-05	3.123e-03
1	4.187e-03	1.629e-04	3.318e-02
5	4.160e-03	7.703e-04	1.511e-01
10	4.741e-03	1.512e-03	3.350e-01

Table 1: Conductivity estimation results, continued; Listed in columns are: (i) the distance between $\mathbf{C}_1$ and $\mathbf{C}_1^n$, (ii) the mean estimated conductivity value $\tilde{\sigma}_1^{est}$, (iii) the standard deviation of σ_1^{est}, (iv) the mean value of the relative errors between σ_1 and σ_1^{est}.

cordance with the stability result of Proposition 3.3. In order to penalize high frequencies and to get more accurate estimations, we will in particular introduce in the above criterion (16) appropriate multiplicative weights (decreasing with the index k).

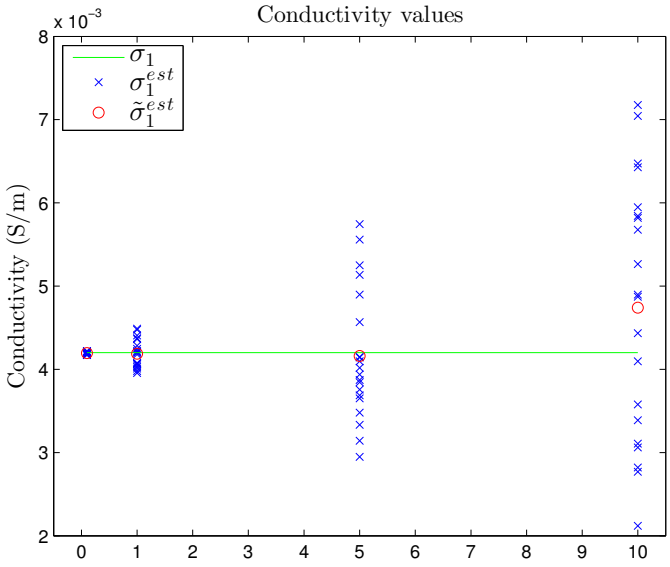

Figure 3: Conductivity estimation results for various mislocations of the actual dipole used to simulate the EEG data: 20 dipole locations $\mathbf{C}_1^n$ are selected by displacing $\mathbf{C}_1$ by a constant distance, computed as a percent of the brain radius r_0 (on the abcissa axis). Displayed are: σ_1, the actual conductivity value used in the EEG data simulation, σ_1^{est}, the estimated conductivity value for each dipole position $\mathbf{C}_1^n$, and $\tilde{\sigma}_1^{est}$, the mean value of σ_1^{est} among $n = 1, \cdots, 20$.

5. Conclusion

Observe that our uniqueness result, Theorem 3.1, may be expressed as an identifiability property of the conductivity value (model parameter) σ_1 in the relation (transfer function) from boundary data to sources (control to observation), [12, 26]. This could be useful in order to couple EEG with additional modalities, like EIT (where $\partial_n u \neq 0$ is known on Γ) or even MEG (magnetoencephalography, which measures the magnetic field outside the head), and to simultaneously estimate both σ_1 and the source term $\mathcal{S}$ in situations where the latter is (partially) unknown.

Following Remark 3.2, we may also wish to recover possibly unknown information about the (spherical) geometry of Ω_1 (like r_1 or/and r_0).

Situations with more than 3 spherical layers could be described similarly, which may help to consider more general conductivities (smooth but non constant) by piecewise constant discretization.

As Theorem 3.1, Proposition 3.3 would still hold true under a weaker sufficient condition for the source terms, according to which the associated potential on S_0 through (5) should admit at least 2 non-null coefficients (this is equivalent to the same property for g on S_2, see Remark 3.2). Moreover, it could be extended to a stability property with respect to boundary data with close and non vanishing Neumann data on S_2. However, stability properties for situations with partial Dirichlet boundary data only (on $\Gamma \subset S_2$) would be weaker, see e.g. [8, 5, 14].

We have also begun to study the same uniqueness and stability issues in more general (non-spherical) nested geometries, see [7, 22, 23, 27], and also [4] for a number of open problems.

6. Acknowledgement

This work was partly supported by the Région Provence-Alpes-Côte d'Azur (France) and the company BESA GmbH (Germany).

Appendix: More computations related to Section 3.2.2

From (11), (12), we get for all $k \geq 0$,

$$\beta_{0k} = g_k \times$$

$$[0\ 1]\, T_k(r_0)^{-1}\, \Sigma_0^{-1}\, \Sigma_1\, T_k(r_0)\, T_k(r_1)^{-1}\, \Sigma_1^{-1}\, \Sigma_2\ T_k(r_1)\, T_k(r_2)^{-1} \begin{bmatrix} 1 \\ 0 \end{bmatrix}.$$

The matrices $T_k(r_i)$ and $T_k(r_i)^{-1}$ can be written:

$$T_k(r_i) = \begin{bmatrix} 1 & 0 \\ 0 & \frac{1}{r_i} \end{bmatrix} \begin{bmatrix} 1 & 1 \\ k & -(k+1) \end{bmatrix} \begin{bmatrix} r_i^k & 0 \\ 0 & r_i^{-(k+1)} \end{bmatrix},$$

$$T_k(r_j)^{-1} = \frac{1}{2k+1} \begin{bmatrix} r_j^{-k} & 0 \\ 0 & r_j^{(k+1)} \end{bmatrix} \begin{bmatrix} k+1 & 1 \\ k & -1 \end{bmatrix} \begin{bmatrix} 1 & 0 \\ 0 & r_j \end{bmatrix}.$$

Their products that give an expression of $\mathcal{T}(S_{i-1}, S_i)$ in the spherical geometry are then such that:

$$T_k(r_{i-1})\, T_k(r_i)^{-1} = \frac{1}{2k+1} \times$$

$$\begin{bmatrix} 1 & 0 \\ 0 & r_{i-1}^{-1} \end{bmatrix} \begin{bmatrix} 1 & 1 \\ k & -(k+1) \end{bmatrix} \begin{bmatrix} \left(\frac{r_{i-1}}{r_i}\right)^k & 0 \\ 0 & \left(\frac{r_i}{r_{i-1}}\right)^{k+1} \end{bmatrix} \begin{bmatrix} k+1 & 1 \\ k & -1 \end{bmatrix} \begin{bmatrix} 1 & 0 \\ 0 & r_i \end{bmatrix}$$

$$= \frac{1}{2k+1}\left(\frac{r_i}{r_{i-1}}\right)^{k+1} \times$$

$$\begin{bmatrix} 1 & 0 \\ 0 & r_{i-1}^{-1} \end{bmatrix} \begin{bmatrix} 1 & 1 \\ k & -(k+1) \end{bmatrix} \begin{bmatrix} \left(\frac{r_{i-1}}{r_i}\right)^{2k+1} & 0 \\ 0 & 1 \end{bmatrix} \begin{bmatrix} k+1 & 1 \\ k & -1 \end{bmatrix} \begin{bmatrix} 1 & 0 \\ 0 & r_i \end{bmatrix}.$$

. We can write

$$T_k(r_{i-1})\, T_k(r_i)^{-1} = \rho_k^{(i)} \begin{bmatrix} a_k^{(i)} & b_k^{(i)} \\ c_k^{(i)} & d_k^{(i)} \end{bmatrix},$$

with

$$\rho_k^{(i)} = \frac{1}{2k+1}\left(\frac{r_i}{r_{i-1}}\right)^{k+1},\ i=1,2\,,\ \rho_k^{(0)} = \frac{r_0^{k+1}}{2k+1}\,,$$

and the real valued quantities, with their equivalent asymptotic behaviours as $k \to \infty$:

$$\begin{cases} a_k^{(i)} = (k+1)\left(\frac{r_{i-1}}{r_i}\right)^{2k+1} + k & \sim k\,, \\ b_k^{(i)} = r_i\left[\left(\frac{r_{i-1}}{r_i}\right)^{2k+1} - 1\right] & \sim -r_i\,, \\ c_k^{(i)} = \frac{k\,(k+1)}{r_{i-1}\,r_i}\, b_k^{(i)} & \sim -\frac{k^2}{r_{i-1}}\,, \\ d_k^{(i)} = \frac{r_i}{r_{i-1}}\left[k\left(\frac{r_{i-1}}{r_i}\right)^{2k+1} + k + 1\right] & \sim \frac{k r_i}{r_{i-1}}\,. \end{cases}$$

Define also the real valued quantities $e_k^{(0)}$, $f_k^{(0)}$:

$$e_k^{(0)} = k\,,\ f_k^{(0)} = f^{(0)} = -r_0\,.$$

We have

$$[0\ 1]\, T_k(r_0)^{-1} = \rho_k^{(0)} \begin{bmatrix} e_k^{(0)} & f_k^{(0)} \end{bmatrix}.$$

Then, equation (13) holds true with:

$$B_1(k) = \frac{\sigma_0}{\rho_k^{(0)}\,\rho_k^{(1)}\,\rho_k^{(2)}} \text{ whence } r_0^{k+1}\, B_1(k) = \sigma_0\,(2k+1)^3\left(\frac{r_0}{r_2}\right)^{k+1} \sim 8k^3\left(\frac{r_0}{r_2}\right)^{k+1},$$

and

$$\begin{cases} A_1(k) = \sigma_0\, e_k^{(0)}\, a_k^{(1)}\, a_k^{(2)} + \sigma_2\, f_k^{(0)}\, d_k^{(1)}\, c_k^{(2)} & \sim k^3(\sigma_0+\sigma_2)\,, \\ A_2(k) = f_k^{(0)}\, c_k^{(1)}\, a_k^{(2)} & \sim k^3\,, \\ A_0(k) = \sigma_0\,\sigma_2\, e_k^{(0)}\, b_k^{(1)}\, c_k^{(2)} & \sim k^3\sigma_0\sigma_2\,. \end{cases}$$

Observe that $r_0^{k+1}\, B_1(k)$ acts on $r_0^{-(k+1)}\, \beta_{0k}$ that are members of an l^2 sequence (see Section 3.2.1 and equation (10) with $i = 0$).

As in (14), one can show with the above expressions that the behaviours of the ratios $A_i(k)/A_2(k)$, $B_1(k)/A_2(k)$ ensure that they all are uniformly bounded from below on from above by positive constants, for $k > 0$.

Note also that

$$\begin{cases} B_1(k) = \sigma_0\, \tilde{B}_1(k)\,, \\ A_1(k) = \sigma_0\, \tilde{A}_{10}(k) + \sigma_2\, \tilde{A}_{12}(k)\,, \\ A_2(k) = \tilde{A}_2(k)\,, \\ A_0(k) = \sigma_0\, \sigma_2\, \tilde{A}_0(k)\,, \end{cases}$$

where $\tilde{A}_i$, $\tilde{A}_{ij}$, $\tilde{B}_1$ only depend on the spherical geometry.

References

[1] G. Alessandrini, *Singular solutions of elliptic equations and the determination of conductivity by boundary measurements*, J. Differential Equations **84** (1990), 252–272.

[2] G. Alessandrini, *Stable determination of conductivity by boundary measurements*, Appl. Anal. **27** (1998), 153–172.

[3] G. Alessandrini, *Generic uniqueness and size estimates in the inverse conductivity problem with one measurement*, Le Matematiche **54** (1999), no. 3, 5–14.

[4] G. Alessandrini, *Open issues of stability for the inverse conductivity problem*, J. Inv. Ill-Posed Problems **15** (2007), 1–10.

[5] G. Alessandrini, L. Rondi, E. Rosset, and S. Vessella, *The stability for the Cauchy problem for elliptic equations*, Inverse Problems **25** (2009).

[6] G. Alessandrini and S. Vessella, *Lipschitz stability for the inverse conductivity problem*, Advances in Applied Mathematics **35** (2005), 207–241.

[7] H. Ammari and H. Kang, *Polarization and moment tensors, with applications to inverse problems and effective medium theory*, Springer, 2007.

[8] B. Atfeh, L. Baratchart, J. Leblond, and J. R. Partington, *Bounded extremal and Cauchy-Laplace problems on the sphere and shell*, J. Fourier Analysis and Applications **16** (2010), no. 2, 177–203.

[9] S. Axler, P. Bourdon, and W. Ramey, *Harmonic function theory*, Springer-Verlag, 2001.

[10] L. Baratchart, A. Ben Abda, F. Ben Hassen, and J. Leblond, *Recovery of pointwise sources or small inclusions in 2D domains and rational approximation*, Inverse problems **21** (2005), 51–74.

[11] H. Brezis, *Analyse fonctionnelle*, Masson, 1987.

[12] G. Chavent and K. Kunisch, *The output least squares identifiability of the diffusion coefficient from an H^1 observation in a 2D elliptic equation*, ESAIM: Control, Optimisation and Calculus of Variations **8** (2002), 423–440.
[13] G. Chen and J. Zhou, *Boundary elements methods*, Academic Press, 1992.
[14] M. Clerc, J. Leblond, J.-P. Marmorat, and T. Papadopoulo, *Source localization using rational approximation on plane sections*, Inverse Problems **28** (2012), no. 5, 055018.
[15] R. Dautray and J.-L. Lions, *Analyse mathématique et calcul numérique*, vol. 2, Masson, 1987.
[16] A. El Badia and T. Ha-Duong, *An inverse source problem in potential analysis*, Inverse Problems **16** (2000), 651–663.
[17] M. Hämäläinen, R. Hari, J. Ilmoniemi, J. Knuutila, and O. V. Lounasmaa, *Magnetoencephalography theory, instrumentation, and applications to noninvasive studies of the working human brain*, Revies of Modern Physics **65** (1993), 413–497.
[18] M. Hämäläinen and J. Sarvas, *Realistic conductivity geometry model of the human head for interpretation of neuromagnetic data*, IEEE Trans. Biomedical Engineering **2** (1989), no. 36, 165–171.
[19] V. Isakov, *On uniqueness of recovery of a discontinuous conductivity coefficient*, Comm. Pure Appl. Math. **41** (1988), 865–877.
[20] V. Isakov, *Inverse problems for partial differential equations*, Springer-Verlag, 1998.
[21] D. Kandaswamy, T. Blu, and D. Van De Ville, *Analytic sensing for multilayer spherical models with application to EEG source imaging*, Inverse Problems and Imaging **7** (2013), no. 4, 1251–1270.
[22] H. Kang and J. K. Seo, *Layer potential technique for the inverse conductivity problem*, Inverse Problems **12** (1996), 267–278.
[23] H. Kang and J. K. Seo, *A note on uniqueness and stability for the inverse conductivity problem with one measurement*, J. Korean Math. Soc. **38** (2001), 781–792.
[24] C. Kenig, J. Sjöstrand, and G. Uhlmann, *The Calderón problem with partial data*, Ann. of Math. **165** (2007), no. 2, 567–591.
[25] A. Kirsch, *An introduction to the mathematical theory of inverse problems*, Springer, 1996.
[26] J. Leblond, *Identifiability properties for inverse problems in EEG data processing and medical engineering, with observability and optimization issues*, Acta Applicandae Mathematicae **135** (2015), no. 1, 175–190.
[27] J. C. Nédélec, *Acoustic and electromagnetic equations integral representations for harmonic problems*, Springer, 2001.
[28] P. L. Nunez and R. Srinivasan, *Electric fields of the brain: the neurophysics of EEG*, Oxford University Press, 2006.
[29] G. Uhlmann, *Electrical impedance tomography and Calderón's problem*, Inverse Problems **25** (2009), no. 12, 123011.
[30] S. Vallaghé and M. Clerc, *A global sensitivity analysis of three- and four-layer EEG conductivity models*, IEEE Transactions on Biomedical Engineering **56** (2009), no. 4, 988–995.

Authors' addresses:

Maureen Clerc
Centre de Recherche Inria Sophia Antipolis - Méditerranée
2004, route des Lucioles - BP 93
06902 Sophia Antipolis Cedex, France
E-mail: maureen.clerc@inria.fr

Juliette Leblond
Centre de Recherche Inria Sophia Antipolis - Méditerranée
2004, route des Lucioles - BP 93
06902 Sophia Antipolis Cedex, France
E-mail: juliette.leblond@inria.fr

Jean-Paul Marmorat
Centre de Mathématiques Appliquées
CS 10207 - 1, rue Claude Daunesse
F-06904 Sophia Antipolis Cedex
E-mail: jean-paul.marmorat@mines-paristech.fr

Christos Papageorgakis
Centre de Recherche Inria Sophia Antipolis - Méditerranée
2004, route des Lucioles - BP 93
06902 Sophia Antipolis Cedex, France
E-mail: christos.papageorgakis@inria.fr

Received April 15, 2016
Revised Month dd, yyyy